

## Impact of Saharan Dust on Tropical North Atlantic SST\*

GREGORY R. FOLTZ

*Joint Institute for the Study of the Atmosphere and Ocean, University of Washington, Seattle, Washington*

MICHAEL J. MCPHADEN

*NOAA/Pacific Marine Environmental Laboratory, Seattle, Washington*

(Manuscript received 11 September 2007, in final form 13 December 2007)

### ABSTRACT

A combination of satellite and in situ datasets is used to investigate the impact of interannual changes in atmospheric dust content on the sea surface temperature (SST) of the tropical North Atlantic Ocean. Throughout most of the region the authors find, in agreement with previous studies, that positive anomalies of dust are associated with a significant reduction in surface shortwave radiation (SWR), while negative anomalies of dust are associated with an enhancement of SWR. Statistical analysis for 1984–2000 suggests that changes in dustiness in the tropical North Atlantic (10°–25°N, 20°–60°W) explained approximately 35% of the observed interannual SST variability during boreal summer, when climatological dust concentrations are highest. Measurements from a long-term moored buoy in the central tropical North Atlantic are used to investigate the causes of anomalously cool SST that occurred in conjunction with a period of enhanced dustiness at the start of the unexpectedly quiet 2006 hurricane season. It is found that surface SWR varied out of phase with dustiness, consistent with historical analyses. However, most of the anomalous cooling occurred prior to the period of enhanced dustiness and was driven primarily by wind-induced latent heat loss, with horizontal oceanic heat advection and SWR playing secondary roles. These results indicate that dust-induced changes in SWR did not play a major direct role in the cooling that led up to the 2006 Atlantic hurricane season.

### 1. Introduction

During boreal summer easterly winds over Africa and the eastern tropical North Atlantic transport  $\sim 1.4 \times 10^{11}$  kg of dust westward several thousands of kilometers over the tropical North Atlantic Ocean (e.g., Prospero and Lamb 2003; Kaufman et al. 2005; Fig. 1a). The dust that remains in the atmosphere affects solar radiation directly through scattering and absorption (Li et al. 2004) and indirectly through its interaction with clouds (Mahowald and Kiehl 2003; Wong and Dessler 2005; Kaufman et al. 2005). The direct effect tends to decrease the amount of solar radiation reaching the

ocean's surface (Li et al. 2004). The overall impact of the indirect effect on surface radiation is less clear since Saharan dust tends to increase low-level cloudiness but may suppress deep convection (Mahowald and Kiehl 2003; Kaufman et al. 2005).

Sea surface temperature (SST) of the tropical North Atlantic Ocean plays an important role in weather and climate, mainly through its effects on rainfall in Northeast Brazil and sub-Saharan Africa (Lamb 1978; Hastenrath and Greischar 1993; Giannini et al. 2003), and tropical cyclone formation and intensification within the Atlantic basin (Saunders and Harris 1997; Shapiro and Goldenberg 1998; Goldenberg et al. 2001; Latif et al. 2007). Previous studies have attributed interannual and decadal SST variability in the tropical North Atlantic mainly to changes in wind-induced latent heat loss, with shortwave radiation (SWR) and horizontal oceanic heat advection playing important secondary roles (Carton et al. 1996; Czaja et al. 2002; Foltz and McPhaden 2006a,b).

During the first half of 2006 SST was above normal throughout most of the tropical North Atlantic (Bell et

---

\* Pacific Marine Environmental Laboratory Contribution Number 3166 and Joint Institute for the Study of the Atmosphere and Ocean Contribution Number 1455.

---

*Corresponding author address:* Gregory R. Foltz, Joint Institute for the Study of the Atmosphere and Ocean, University of Washington, Seattle, WA 98115.  
E-mail: gregory.foltz@noaa.gov

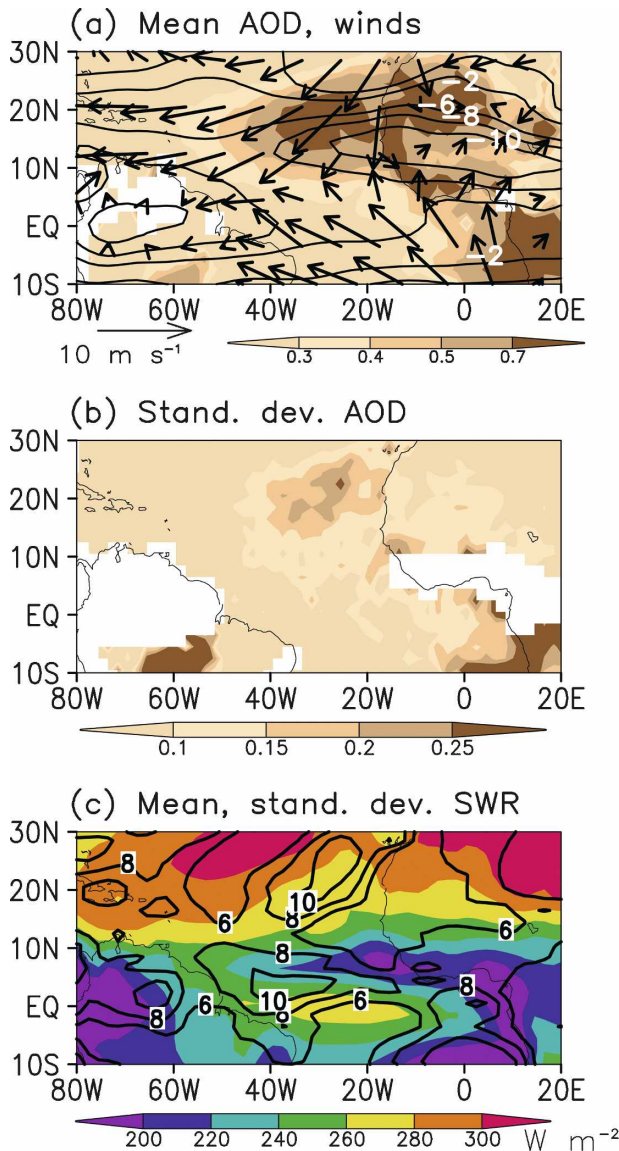


FIG. 1. (a) June–August 1984–2000 mean aerosol optical depth (shaded), surface wind velocity (arrows), and 600-hPa zonal wind speed (contours,  $\text{m s}^{-1}$ ). White shading indicates regions without data owing to persistent cloud cover. (b) Standard deviation of JJA AOD. White shading indicates regions with insufficient data ( $<5$  JJA means). (c) JJA mean surface shortwave radiation (shaded) and standard deviation of JJA SWR (contours,  $\text{W m}^{-2}$ ).

al. 2007). Warm SSTs combined with low vertical wind shear led many forecasters to predict above-normal tropical cyclone activity in 2006 following record activity in 2005 (12 tropical storms and 15 hurricanes, Bell et al. 2006). The 2006 season was significantly quieter than anticipated, however, with only four tropical storms and five hurricanes developing. The sharp reduction in activity in 2006 has been attributed mainly to a late-developing El Niño event (McPhaden 2008), which en-

hanced vertical wind shear in the tropical North Atlantic and Caribbean during September and October 2006 (Bell et al. 2007).

Lau and Kim (2007a,b) suggest that changes in atmospheric dust concentration also may have played a significant role in suppressing tropical cyclone activity in the western tropical North Atlantic during 2006. They argue that an anomalous increase in dust loading during June 2006 triggered SST cooling through coupled air–sea interaction, leading to an environment less favorable for tropical cyclone development. In contrast, Evan (2007) argues that the changes in dustiness during 2006 were not large enough to significantly affect SST. On a broader scale, Schollaert and Merrill (1998) used historical satellite estimates of dust and in situ SST for the month of July to show that changes in dust content in the eastern and central tropical North Atlantic are associated with a significant reduction in the underlying SST.

The aforementioned studies are incomplete regarding the impact of changes in dustiness on tropical North Atlantic SST. For example, Lau and Kim (2007a,b) made arguments based on observed changes in dust content and SST during 2005–06 only, together with estimates of the climatological mixed layer depth (MLD). Evan’s (2007) analysis also relied on a mixed layer depth climatology together with a qualitative comparison of changes in dustiness and SST during the 1980s and 1990s. The analysis region of Schollaert and Merrill (1998) was limited to narrow ship tracks in the eastern and western tropical North Atlantic, and the time period they considered covered only four years. None of the aforementioned studies performed an explicit oceanic mixed layer heat budget analysis.

In this study we use  $\sim 15$  yr of satellite aerosol, shortwave radiation, and SST data to examine the impact of interannual changes in atmospheric dust content on the SST of the tropical North Atlantic Ocean. We expand on the results of Schollaert and Merrill (1998) through the use of a combined satellite–in situ SST product, which offers enhanced spatial and temporal coverage with respect to in situ observations. We also use in situ measurements from a long-term moored buoy in the central tropical North Atlantic Ocean, together with satellite estimates of dust concentration, to examine the impact of increased dust loading on SST leading up to the 2006 Atlantic hurricane season. We consider the mixed layer heat budget at the mooring location, expanding on the analyses of Lau and Kim (2007a,b) and Evan (2007).

## 2. Data

A variety of satellite and in situ datasets is used in this study. Aerosol optical depth (AOD) at 380 nm was

obtained from the Total Ozone Mapping Spectrometer (TOMS) on board the *Nimbus-7* and *Earth Probe* satellites and is used as a proxy for total atmospheric dust content (e.g., Torres et al. 1998, 2002). These data are available as monthly averages on a  $1^\circ \times 1^\circ$  grid. The *Nimbus-7* data cover the period January 1980–April 1993, and the *Earth Probe* data are available during August 1996–December 2001. Data from 2001 are excluded owing to a spurious drift in the *Earth Probe* TOMS (Kiss et al. 2007). We also use AOD measurements at 550 nm from the Moderate Resolution Imaging Spectroradiometer (MODIS) on board the *Terra* satellite (e.g., Remer et al. 2005). This dataset consists of monthly means on a  $1^\circ \times 1^\circ$  grid for February 2000–May 2007. Measurements from TOMS and MODIS correspond reasonably well to ground-based measurements of AOD (Hsu et al. 1999; Remer et al. 2005). Satellite-based estimates of AOD include contributions from absorbing aerosols such as smoke and soot in addition to soil dust. However, over the tropical and subtropical North Atlantic the aerosol load is dominated by soil dust originating from North Africa (Li et al. 1996; Tegen et al. 1997; Chiapello et al. 1999).

We also use estimates of surface shortwave radiation that are based on satellite measurements from the International Cloud Climatology Project (ISCCP) (Rossow and Duenas 2004) and a radiative transfer model (Zhang et al. 2004). This dataset is available on a  $2.5^\circ \times 2.5^\circ$  grid for July 1983–December 2004. Interannual variations of aerosol concentration are not included explicitly but are present indirectly through the classification of dust as low cloudiness in the ISCCP dataset (Zhang et al. 2004; Evan et al. 2006).

Monthly surface and 600-hPa wind velocity data were obtained from the National Centers for Environmental Prediction–Department of Energy (NCEP–DOE) reanalysis-2 (hereafter NCEP2), available on a  $2^\circ \times 2^\circ$  grid for 1979–2006 (Kanamitsu et al. 2002). We also use daily surface wind velocity from the SeaWinds scatterometer on board the Quick Scatterometer (QuikSCAT) satellite. This dataset is on a  $0.25^\circ \times 0.25^\circ$  grid and is available for 1999–2006. Two different SST products are analyzed in this study: The first is a combined satellite–in situ product, available monthly on a  $1^\circ \times 1^\circ$  grid for 1981–present (Reynolds et al. 2002), and the second is from the Tropical Rainfall Measuring Mission (TRMM) Microwave Imager (TMI), available daily on a  $0.5^\circ \times 0.5^\circ$  grid beginning December 1997 (Wentz 1997).

Horizontal ocean currents were obtained from the Ocean Surface Currents Analysis—Real Time (OSCAR). This product calculates velocity averaged in the upper

30 m of the water column using a diagnostic model and satellite estimates of surface wind stress, sea level, and SST (Bonjean and Lagerloef 2002). The dataset is available on a  $1^\circ \times 1^\circ$  grid every five days beginning October 1992 and is interpolated to a daily resolution for use with the mooring data described below.

In situ measurements were obtained from the northernmost moored buoy site of the Pilot Research Array in the Tropical Atlantic (PIRATA) (Servain et al. 1998) located at  $15^\circ\text{N}$ ,  $38^\circ\text{W}$ . Measurements, begun in 1998 and continued through the present, include subsurface temperature and salinity, air temperature, relative humidity, wind velocity, shortwave radiation, and precipitation. From 1998 to June 2005, ocean temperature was measured at 11 depths between 1 and 500 m, with 20-m spacing in the upper 140 m, while salinity was measured at 1 m, 20 m, 40 m, and 120 m at all moorings. Beginning in July 2005, additional temperature measurements have been made at 10 and 13 m and additional salinity measurements at 10 and 60 m. Air temperature and relative humidity are measured at a height of 3 m MSL, shortwave radiation and rainfall are measured at 3.5 m, and wind velocity at 4 m. Daily averages are transmitted to shore in real time, while high temporal resolution data (1–10-min averages) are internally recorded. Here we use the daily averaged data for January 2000–December 2006.

The NCEP2 surface and 600-hPa wind velocity, together with TOMS AOD and the SWR dataset, are used to examine mean conditions and interannual variability in the tropical North Atlantic during boreal summer when atmospheric dust concentrations are highest (Fig. 1). The SWR data, in combination with the AOD and SST datasets, are used in section 3 to examine the relationships between dustiness, SWR, and SST on interannual time scales, focusing on the time period July 1983–December 2000 when all datasets are available. Finally, QuikSCAT wind velocity, MODIS AOD, TMI SST, OSCAR currents, and PIRATA mooring data are used in section 4 to examine the conditions in the tropical North Atlantic during October 2004–September 2006, a period characterized by significant interannual variations of dustiness and SST (e.g., Foltz and McPhaden 2006a; Lau and Kim 2007a). We also use these data to analyze the mixed layer heat budget at the PIRATA mooring location in order to assess the causes of the anomalous SST cooling leading up to the 2006 hurricane season.

### 3. Results

In this section we examine the relationships between AOD, SWR, and SST in the tropical North Atlantic.

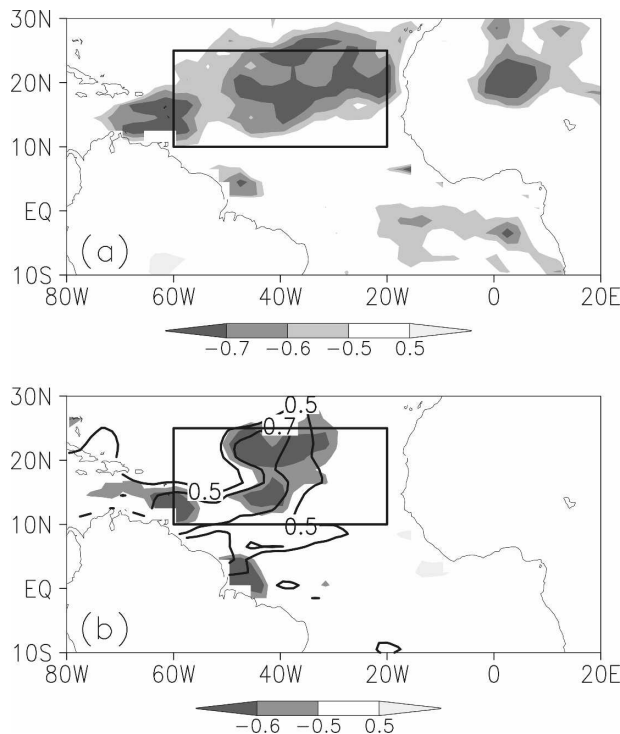


FIG. 2. (a) Linear correlation coefficients for AOD and surface SWR (shaded). Values are for JJA means for 1984–2000. (b) As in (a) but for SWR and  $\partial(\text{SST})/\partial t$  (shaded) and for AOD and  $\partial(\text{SST})/\partial t$  (contours). Shading/contours are shown only where the correlations are significant at the 10% level. Boxes enclose regions used to form averages shown in Figs. 4 and 5.

We begin by considering mean conditions during boreal summer when dust rises several kilometers into the atmosphere over the Sahara and Sahel. The atmospheric circulation during this season is influenced by the northeasterly trade winds near the surface and the African easterly jet (AEJ) centered near 600 mb over western Africa (Fig. 1a). Some of the dust is therefore advected westward by the AEJ and trade winds, resulting in a region of enhanced AOD ( $>0.3$ ) over most of the tropical North Atlantic (Prospero and Carlson 1972; Fig. 1a). High values of AOD south of  $\sim 10^\circ\text{N}$  are associated mainly with smoke from biomass burning (e.g., Chatfield et al. 1998). Surface shortwave radiation is greatest in the subtropical North Atlantic and North Africa and reaches minima over the Amazon and in the  $0^\circ$ – $10^\circ\text{N}$  latitude band of the ITCZ (Fig. 1c).

To assess the impact of changes in dustiness on the underlying SST, we first consider the interannual variability of AOD and SWR. Anomaly time series for each variable are formed by removing the corresponding monthly mean seasonal cycle at each grid point. We find that interannual variations of AOD are strongest in the northeastern tropical North Atlantic where the

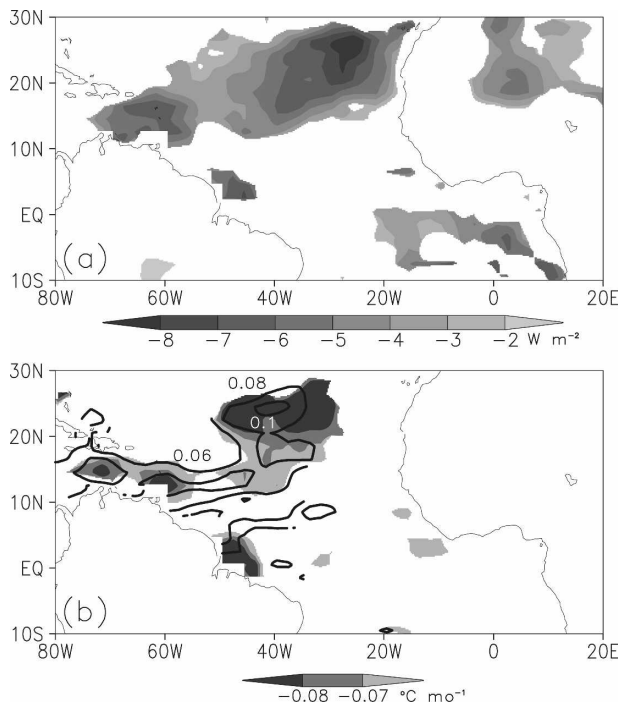


FIG. 3. (a) JJA means of SWR regressed onto AOD. (b) As in (a), except for  $\partial(\text{SST})/\partial t$  regressed onto SWR (contours,  $^\circ\text{C mo}^{-1}$ ) and  $\partial(\text{SST})/\partial t$  regressed onto AOD (shaded). Regression of SWR onto AOD has been normalized by one standard deviation of AOD. Regression of  $\partial(\text{SST})/\partial t$  onto SWR has been normalized by one standard deviation of SWR. Shading/contours are shown only where the regression coefficients are significant at the 10% level.

boreal summer mean AOD is high (Fig. 1b). Variations of SWR are also strongest in the northeastern basin, corresponding to the region of enhanced AOD variability (Fig. 1c).

Next linear correlation and regression analyses are used to quantify the relationships between anomalous AOD, SWR, and SST. The analyses are performed at each grid point using two methods. The first method makes use of all calendar months, and the second uses only the June–August (JJA) mean from each year, corresponding to the season when climatological dust content is highest. Significance of the correlation and regression coefficients for each method is assessed using the 90% confidence level of a 1000-sample bootstrap test (Wilks 1995). We have found that the spatial patterns and significance of the correlation and regression coefficients are similar for each method. We therefore discuss in detail only the JJA analyses, when the signals are strongest (Figs. 2–4), and summarize the results for all months in Table 1.

Throughout most of the tropical North Atlantic SWR anomalies are significantly negatively correlated with AOD anomalies, suggesting that enhanced (dimin-

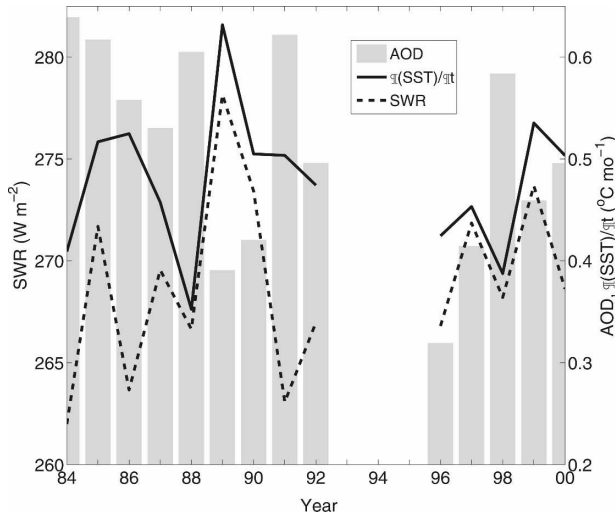


FIG. 4. JJA mean AOD (shaded),  $\partial(\text{SST})/\partial t$  (solid), and SWR (dashed) averaged in the tropical North Atlantic ( $10^{\circ}$ – $25^{\circ}$ N,  $20^{\circ}$ – $60^{\circ}$ W; Fig. 2 shows the averaging region).

ished) dustiness is associated with a reduction (increase) in SWR (Fig. 2a). These results are consistent with those of previous studies (e.g., Li et al. 2004). The relationship is strongest in the eastern half of the basin, where the boreal summer mean and interannual variability of AOD are high (Figs. 1a,c).

During boreal summer interannual fluctuations of SWR are significantly positively correlated with changes in  $\partial(\text{SST})/\partial t$  (which for shorthand we will write as  $\text{SST}_t$ ) in the central tropical North Atlantic, suggesting that in this region SWR may be an important driver of SST (i.e., Foltz and McPhaden 2006a,b; Fig. 2c). Negative correlations between AOD and SWR are also strong in this region (Fig. 2a). As a result, changes in AOD are associated with significant cooling of the underlying SST that is confined mainly to the central tropical North Atlantic ( $30^{\circ}$ – $50^{\circ}$ W). In this region interannual variations of dust content locally explain up to 50% of the observed  $\text{SST}_t$  variability during JJA based on the AOD– $\text{SST}_t$  correlation coefficients.

To quantify the relationships between AOD, SWR, and  $\text{SST}_t$  further, we consider the linear regression coefficients between these terms (Fig. 3). To facilitate comparison between regression coefficients and to account for spatial variations in the strengths of interannual AOD and SWR fluctuations, regression coefficients are expressed in terms of a one standard deviation change in the independent variable (Fig. 1 shows the magnitude of a one standard deviation change in AOD and SWR). We find that an increase of one standard deviation in AOD is associated with a maximum decrease in SWR of  $8 \text{ W m}^{-2}$  off the coast of northwest

TABLE 1. Regression and correlation coefficients (in parentheses) for quantities averaged in the tropical North Atlantic ( $10^{\circ}$ – $25^{\circ}$ N,  $20^{\circ}$ – $60^{\circ}$ W). First column: Shortwave radiation anomalies (SWR) regressed onto aerosol optical depth anomalies (AOD) ( $\text{W m}^{-2}$ ). Second column: Reynolds et al. (2002)  $\partial(\text{SST})/\partial t$  anomalies ( $\text{SST}_t$ ) regressed onto SWR ( $^{\circ}\text{C month}^{-1}$ ). Third column:  $\text{SST}_t$  regressed onto AOD ( $^{\circ}\text{C month}^{-1}$ ). Coefficients are shown for all calendar months and for June–August only, and with and without linear trends included. All regression coefficients correspond to a one standard deviation change in the independent variable (second one listed in each column heading). For all months these standard deviations are 0.05 for AOD with and without the linear trend included, and  $5 \text{ W m}^{-2}$  ( $4 \text{ W m}^{-2}$ ) for SWR with (without) the trend. For July–August the standard deviations are 0.1 (0.05) for AOD with (without) the trend included, and  $5 \text{ W m}^{-2}$  ( $4 \text{ W m}^{-2}$ ) for SWR with (without) the trend. Bold indicates significance at the 10% level.

	SWR, AOD	$\text{SST}_t$ , SWR	$\text{SST}_t$ , AOD
All months			
Trend included	<b>-3 (-0.5)</b>	<b>0.03 (0.4)</b>	<b>-0.01 (-0.2)</b>
Trend removed	<b>-2 (-0.6)</b>	<b>0.03 (0.4)</b>	<b>-0.01 (-0.2)</b>
JJA			
Trend included	<b>-3 (-0.6)</b>	<b>0.04 (0.6)</b>	-0.02 (-0.3)
Trend removed	<b>-3 (-0.7)</b>	<b>0.04 (0.6)</b>	<b>-0.04 (-0.6)</b>

Africa. The regression coefficient decreases southwestward to  $3 \text{ W m}^{-2}$  at  $50^{\circ}$ W, then increases to a secondary maximum near  $60^{\circ}$ W (Fig. 3a). The standardized linear regression coefficients for SWR and AOD correspond to unnormalized values of  $-60$  to  $-40 \text{ W m}^{-2} \text{ AOD}^{-1}$  throughout most of the basin. These values are slightly smaller in magnitude than the  $-65 \text{ W m}^{-2} (\text{AOD})^{-1}$  clear-sky SWR forcing efficiency estimates of Li et al. (2004), which are based on different satellite datasets and model calculations.

A one standard deviation change in AOD is associated with a maximum change in SST of  $\sim 0.07^{\circ}$ – $0.08^{\circ}\text{C month}^{-1}$  in the central basin ( $35^{\circ}$ – $45^{\circ}$ W) and in the eastern Caribbean Sea between  $10^{\circ}$  and  $15^{\circ}$ N (Fig. 3b). A change in SWR of one standard deviation has a similar impact on SST in these regions ( $\sim 0.08^{\circ}$ – $0.12^{\circ}\text{C month}^{-1}$ ), indicating that a significant fraction of the SWR-driven SST variability covaries with changes in atmospheric dust content. The AOD– $\text{SST}_t$  regression coefficients are consistent with the estimate of Evan (2007) for June 2006 in the western Atlantic and Caribbean region ( $0.1^{\circ}\text{C month}^{-1}$ ) and are at the lower end of the range estimated by Lau and Kim (2007b) ( $0.1^{\circ}$ – $0.18^{\circ}\text{C month}^{-1}$ ).

The preceding statistical analyses showed that there were significant relationships between anomalies of AOD, SWR, and  $\text{SST}_t$  during 1983–2000. To examine the temporal evolution of the anomalies during this period and to assess the strengths of the relationships over a broader region, we consider time series of the JJA

anomalies averaged in the tropical North Atlantic ( $10^{\circ}$ – $25^{\circ}$ N,  $20^{\circ}$ – $60^{\circ}$ W). We find that there are significant correlations between the area-averaged AOD, SWR, and SST, anomalies during 1983–2000 (Figs. 4a,b; Table 1). An anomalous increase in AOD is associated with an anomalous decrease in SWR, consistent with Fig. 2. The most striking aspect of the area-averaged time series is a sharp drop in AOD in 1989 that occurs concurrently with increases in SWR and SST, (Fig. 4). The drop in AOD is followed two years later by an increase in AOD and a corresponding decrease in SWR. The higher than normal AOD in 1991 and 1992 is likely related to the eruption of Mount Pinatubo in June 1991. The results of the correlation and regression analyses presented in Table 1 are not significantly changed if these two years are excluded from the analysis.

In addition to considerable interannual variability, there is a downward trend in AOD and an upward trend in SWR. The SWR trend is consistent with the global analysis of Wild et al. (2005), though a more recent analysis suggests the trend may be an artifact of changes in satellite coverage (Evan et al. 2007). The strength of the out-of-phase relationship between AOD and SWR on decadal and longer time scales is therefore highly uncertain. We note, however, that correlation and regression coefficients between SWR, AOD, and SST, are not appreciably changed when linear trends are excluded (Table 1), suggesting that covariability on interannual time scales dominates. The correlation and regression analyses presented earlier in this section (Figs. 2 and 3) are also similar if linear trends in AOD, SWR, and SST are removed, indicating that our results are not highly sensitive to potential long-term drifts in satellite aerosol and cloud retrievals. The relationships between AOD, SWR, and SST, are also stronger when examined for JJA than for all months. For example, when linear trends are excluded interannual variations of AOD explain  $\sim 35\%$  of the SST, variability during JJA and only  $\sim 5\%$  for all months based on the linear correlation coefficients (Table 1).

The preceding analyses are based on a SST product that relies on satellite infrared measurements, which are affected by the presence of aerosols in the atmosphere. It is therefore possible that the significance of the dust–SST relationship has been overestimated since uncorrected SST retrievals would be biased low in the presence of dust (e.g., Nalli and Reynolds 2006). To explore this possibility, we have recomputed the correlation coefficients between AOD and SST, for JJA using TMI SST, which is not influenced by aerosols. Focusing on the time period 2000–06, when MODIS AOD and TMI SST are available, we find that the dust–SST, relationship averaged over the tropical North Atlantic

is slightly stronger when TMI SST is substituted for Reynolds et al. (2002) SST (correlation coefficients of  $-0.2$  and  $-0.1$ , respectively, though neither coefficient is significant at the 10% level because of the relative shortness of the records). The similarity of the correlation coefficients suggests that the observed relationship between dust and SST is real and not an artifact of aerosol and cloud contamination of infrared SST retrievals.

#### 4. Mixed layer heat balance

In this section we use in situ measurements from a PIRATA mooring in the central tropical North Atlantic ( $15^{\circ}$ N,  $38^{\circ}$ W), together with satellite AOD, to investigate the impact of interannual changes in dustiness on SWR and SST. The mooring is within the main development region for hurricanes ( $10^{\circ}$ – $20^{\circ}$ N,  $20^{\circ}$ – $80^{\circ}$ W) (Goldenberg and Shapiro, 1996) and is situated near the center of the African dust plume (Fig. 1a).

During 2000–06 SST, is negatively correlated with AOD at the mooring location ( $-0.3$ , which is significant at the 20% level; Fig. 5), in agreement with the satellite-based results of the previous section. The SST and AOD anomalies at  $15^{\circ}$ N,  $38^{\circ}$ W are well correlated with the corresponding SST and AOD anomalies averaged over the tropical North Atlantic ( $10^{\circ}$ – $25^{\circ}$ N,  $20^{\circ}$ – $60^{\circ}$ W), suggesting that conditions at the mooring were representative of the larger-scale patterns of variability (Fig. 5).

Next we focus on the time period October 2004–September 2006. This period was characterized by record-high warm SST anomalies in early 2005, followed by only slightly above-normal SSTs in 2006 (Foltz and McPhaden 2006a; Lau and Kim 2007a; Fig. 5a). AOD was anomalously low from mid-2004 to early 2005 and anomalously high during boreal summer 2005, coinciding with periods of anomalous SST warming and cooling, respectively (Fig. 5b).

During the second half of 2005 SST cooled considerably in the tropical North Atlantic following record warmth in early 2005 (Fig. 6b). The cooler conditions occurred in conjunction with enhanced AOD and wind speed throughout a large portion of the basin and warmer SST in the eastern equatorial region (Figs. 6b,c). The spatial pattern of the 2006 – 2005 SST difference in the tropical North Atlantic corresponds well to the 2006 – 2005 AOD difference, with enhanced AOD during boreal summer 2006 occurring in conjunction with cooler SST. The direction of the anomalous winds from cooler SST in the north to warmer SST along the equator is suggestive of a coupled wind–evaporation–SST feedback (e.g., Chang et al. 1997).

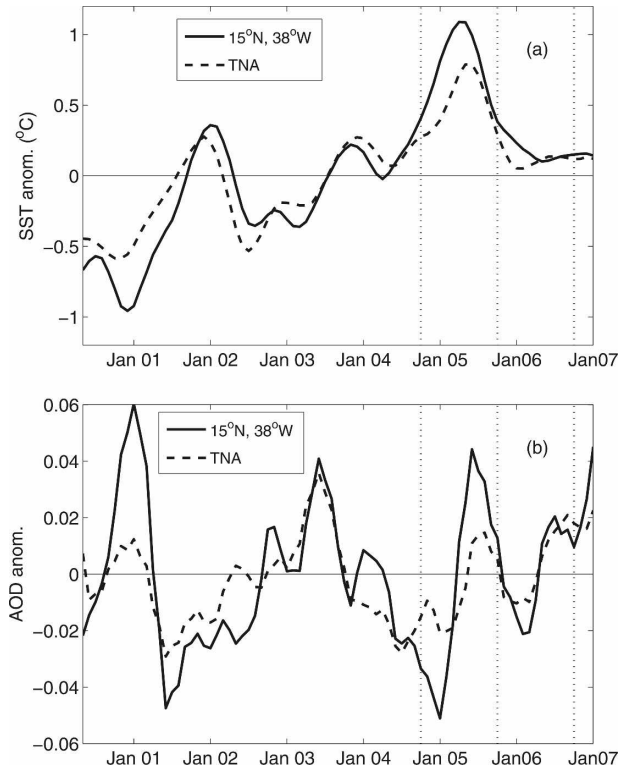


FIG. 5. (a) SST anomalies (with respect to the seasonal cycle) at the PIRATA mooring location ( $15^{\circ}\text{N}$ ,  $38^{\circ}\text{W}$ ; solid line) and averaged in the tropical North Atlantic ( $10^{\circ}$ – $25^{\circ}\text{N}$ ,  $20^{\circ}$ – $60^{\circ}\text{W}$ ; dashed line). Gaps in the PIRATA SST record during October 2004 through July 2005 have been filled with 20-m temperature after application of a seasonal mean offset correction. (b) As in (a) but for MODIS AOD. All time series have been smoothed with successive applications of centered 3-month and 5-month running means. This procedure gives  $\sim 8$ -month low-pass-filtered time series while minimizing negative sidelobes in the frequency response curve and retaining a sufficient number of data points at the ends of the time series (Zhang et al. 1997). Vertical lines in (a) and (b) define time periods used in the heat budget analysis in Fig. 8.

Lau and Kim (2007a,b) argue that changes in dustiness also may have played a significant role. They hypothesize that an increase in dust loading, through direct and coupled air–sea interactions, may have significantly cooled the SST in the western basin ( $40^{\circ}$ – $70^{\circ}\text{W}$ ,  $15^{\circ}$ – $30^{\circ}\text{N}$ ) leading up to the 2006 Atlantic hurricane season.

To investigate the causes of the anomalous cooling between 2005 and 2006 we consider the oceanic mixed layer heat balance at the PIRATA mooring location. Following Moisan and Niiler (1998), the heat balance can be written:

$$\rho c_p h \frac{\partial T}{\partial t} = q_0 - \rho c_p h \mathbf{v} \cdot \nabla T + q_{-h}. \quad (1)$$

The terms in (1) represent, from left to right, mixed layer heat storage rate, surface heat flux corrected for

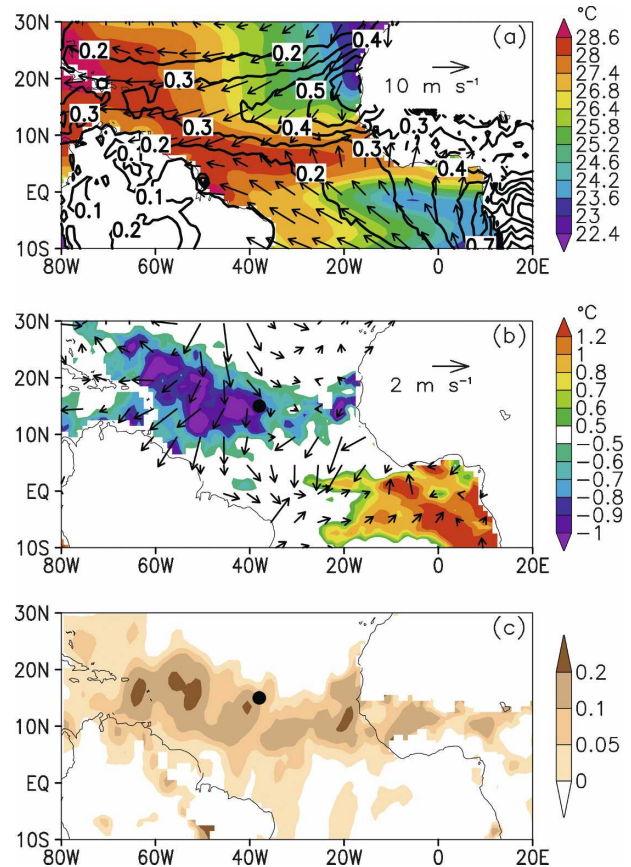


FIG. 6. (a) JJA 2004–06 mean SST (shaded), surface wind velocity (arrows), and AOD (contours). (b) JJA 2006 minus JJA 2005 SST (shaded) and wind vector differences. (c) JJA 2006 minus JJA 2005 AOD difference. Black dot in (b) and (c) denotes location of PIRATA mooring used in this study.

the penetration of shortwave radiation through the base of the mixed layer, horizontal mixed layer heat advection, and vertical entrainment/diffusion at the base of the mixed layer. Here  $h$  is the depth of the mixed layer and  $T$  and  $\mathbf{v}$  are temperature and velocity, respectively, vertically averaged from the surface to a depth of  $-h$ .

We estimate  $h$  and  $T$  from subsurface temperature and salinity at the mooring, using the criterion of a  $0.03 \text{ kg m}^{-3}$  density increase from a depth of 10 m for  $h$  (equivalent to the criterion of a  $0.1^{\circ}\text{C}$  decrease in temperature when salinity is constant with depth). A depth of 10 m is chosen to avoid the shallow diurnal cycle, following de Boyer Montégut et al. (2004). This mixed layer depth criterion results in mixed layers that are significantly shallower than those estimated using the  $0.125 \text{ kg m}^{-3}$  criterion of Monterey and Levitus (1997), for example. Our choice of the  $0.03 \text{ kg m}^{-3}$  criterion is based on several factors. First, in this study we estimate horizontal advection using velocity estimates that are

averaged in the upper 30 m. Using a larger MLD criterion results in MLDs that are significantly greater than 30 m throughout most of the year. This, in turn, may lead to an overestimation of horizontal advection. Second, a shallower mixed layer results in estimates of  $T$  that are closer to SST. This gives more accurate estimations of horizontal mixed layer temperature gradients, which are estimated with SST as a proxy for  $T$ . Finally, prior to July 2005 salinity was measured at depths of 1 m, 20 m, 40 m, and 120 m at the mooring. The lack of measurements between 40 and 120 m during this time period leads to significant uncertainties in MLD when the mixed layer is  $>40$  m. A criterion of  $0.03 \text{ kg m}^{-3}$  gives a MLD that is  $<40$  m throughout most of the year. The sensitivity of the terms in the heat balance to the choice of mixed layer depth criterion is discussed later in this section.

The surface heat flux consists of latent and sensible heat flux, net longwave radiation emission, and shortwave radiation absorption. Latent and sensible heat flux are estimated from the Coupled Ocean–Atmosphere Response Experiment (COARE) bulk flux algorithm (Fairall et al. 2003) with daily buoy estimates of SST, air temperature, relative humidity, and wind speed. The use of daily values instead of 10-min values leads to a negative bias in latent heat flux (LHF) of  $<3 \text{ W m}^{-1}$  (Foltz et al. 2003). This bias is small compared to the typical magnitude of interannual LHF anomalies at the mooring location (discussed later in this section).

Longwave radiation emission is estimated from the Clark et al. (1974) bulk formula following the methodology of Foltz and McPhaden (2005). The net surface shortwave radiation is available directly from the moorings, assuming an albedo of 6%. Following Wang and McPhaden (1999), we model the amount of shortwave radiation penetrating the mixed layer as  $Q_{\text{pen}} = 0.47Q_{\text{sfc}}e^{-h/d_e}$ , where  $Q_{\text{sfc}}$  is the surface shortwave radiation,  $d_e$  is the  $e$ -folding depth of shortwave radiation, and  $h$  is the depth of the mixed layer. Here we assign  $d_e = 25 \text{ m}$  following Wang and McPhaden (1999). The sensitivity of absorbed SWR to the choice of  $d_e$  is discussed later in this section.

Horizontal mixed layer temperature gradients are calculated as a centered difference over a distance of  $3^\circ$  using 3-day running means of TMI SST. These estimates are multiplied by OSCAR currents in order to estimate mixed layer temperature advection. We cannot directly compute the vertical entrainment/diffusion term, but can infer it from the residual of the heat balance.

Uncertainties for the terms in (1) are estimated using

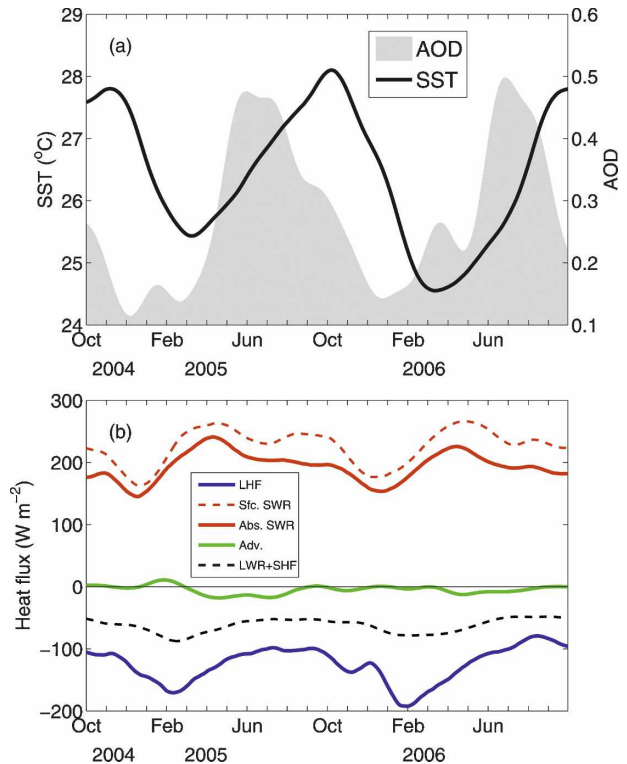


FIG. 7. (a) SST (black line) and AOD (gray shading) at the PIRATA mooring location ( $15^\circ\text{N}$ ,  $38^\circ\text{W}$ ; Figs. 6b,c) during October 2004–September 2006. (b) As in (a) but for latent heat flux (blue), surface shortwave radiation (dashed red), shortwave radiation absorbed in the mixed layer (solid red), horizontal oceanic heat advection (green), and the combination of net longwave radiation emission and sensible heat loss (dashed black). All time series in this and subsequent figures have been smoothed with successive applications of centered 31-day and 41-day running means, resulting in  $\sim 3$ -month low-pass-filtered time series.

instrumental errors for the PIRATA sensors (information available online at [http://www.pmel.noaa.gov/tao/proj\\_over/sensors.shtml](http://www.pmel.noaa.gov/tao/proj_over/sensors.shtml)). We use error estimates for TMI SST and OSCAR currents that are based on comparisons to in situ measurements (see [http://www.esr.org/%7Ebonjean/oscar/global\\_validation/index\\_files/Atlantic.htm](http://www.esr.org/%7Ebonjean/oscar/global_validation/index_files/Atlantic.htm) and Gentemann et al. 2004, respectively). Errors in  $h$  are estimated following Foltz and McPhaden (2008).

Before investigating the causes of the anomalous cooling during late 2005 and early 2006 using (1), we first consider SST, AOD, and surface heat fluxes at the mooring location during this time period (Fig. 7). AOD undergoes a strong annual cycle, with a peak in boreal summer that occurs  $\sim 3$ – $4$  months before the seasonal maximum in SST (Fig. 7a). There is also considerable interannual variability: SST is  $\sim 1^\circ\text{C}$  cooler during early 2006 in comparison to early 2005 and AOD is  $\sim 0.1$  lower (Figs. 5 and 7a). LHF and SWR also exhibit

strong annual cycles, with minima in boreal winter (Fig. 7b). The annual means and seasonal amplitudes of horizontal advection and the combination of longwave radiation emission and sensible heat loss are much weaker in comparison to those of LHF and SWR.

Next, we examine the mixed layer heat balance during October 2004–September 2006. First the 2-yr period is broken into two year-long time series: October 2004–September 2005 (hereafter “2005”) and October 2005–September 2006 (hereafter “2006”). Year 2005 is centered on the peak of the warm anomaly in early 2005, and year 2006 encompasses the subsequent cooler period (Fig. 5). We then calculate daily differences between 2006 and 2005 for each term in (1) (Fig. 8).

Significant cooling occurred during the first half of 2006 relative to 2005 and was caused primarily by changes in LHF, with SWR and horizontal advection playing important secondary roles (Figs. 8a,b). The LHF term was driven primarily by stronger winds during October 2005–February 2006. Anomalous cooling from horizontal advection resulted mainly from mean northward currents acting on a weaker southward SST gradient (i.e., weaker southward SST increase) during October 2005–February 2006 compared to the previous October–February. Changes in LWR and sensible heat flux were insignificant compared to the combined effects of LHF, SWR, and horizontal advection.

Surface SWR was generally stronger in October 2005–January 2006 and April–June 2006 and weaker during February–March 2006 and July–September 2006 compared to the previous year, with absolute differences of up to  $20 \text{ W m}^{-2}$  (Fig. 8a). The largest differences in AOD occurred during February–May and were associated with significant surface SWR differences. AOD was greater during February–March 2006 and SWR was weaker (positive and negative differences, respectively, in Fig. 8a). During April–May the situation was reversed: AOD was weaker during 2006 in comparison to 2005 and surface SWR was greater. The out-of-phase relationship between AOD and SWR during this time period suggests changes in dust content may have contributed significantly to changes in SWR. The correlation between differences in mooring SWR and AOD is  $-0.4$  for the entire year, which is the same sign but slightly weaker in magnitude than the satellite-based SWR–AOD anomaly correlation (Table 1). This correlation is significant only at the 65% confidence level because of the shorter time period considered. However, consistency with our historical analysis suggests a plausible physical connection between the two during 2005–06.

Changes in AOD likely contributed to changes in SST during 2006, consistent with our historical analysis.

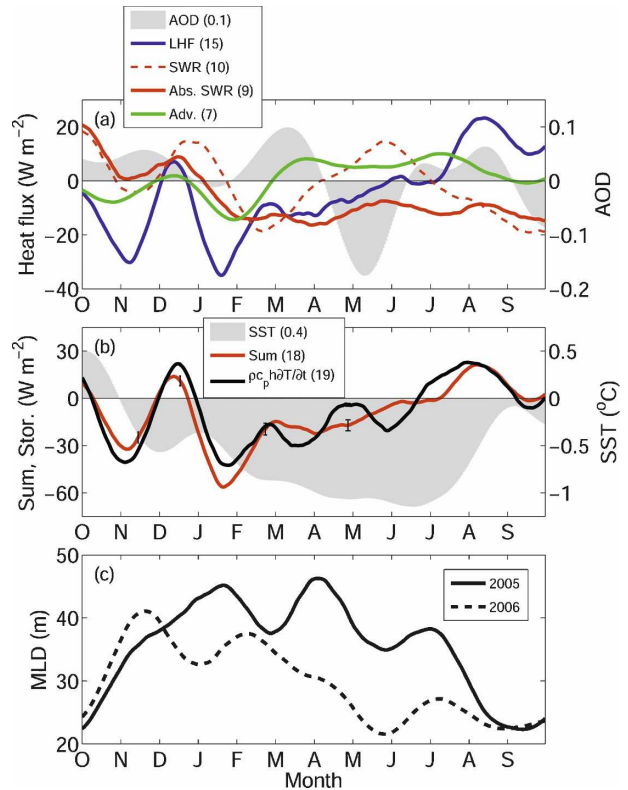


FIG. 8. (a) October 2005–September 2006 minus October 2004–September 2005 differences of AOD (gray shading), LHF (blue), surface SWR (dashed red), SWR absorbed in the mixed layer (solid red), and horizontal heat advection (Adv.; green) at the PIRATA mooring location. (b) As in (a) but for SST (gray shading); sum of LHF, absorbed SWR, and Adv. (black); and mixed layer heat storage rate (red). The standard deviation of each term in (a) and (b) is shown in parentheses in the legend. Black error bars in (b) represent one standard error. (c) Mixed layer depth at the mooring location during October 2004–September 2005 (solid) and October 2005–September 2006 (dashed).

The effect is weaker than the influence of LHF on SST, however, since SWR exerts only a secondary influence on SST (Fig. 8a). For example, the standard deviation of the 2006 minus 2005 LHF difference is  $15 \text{ W m}^{-2}$ , compared to only  $10 \text{ W m}^{-2}$  for surface SWR. In addition, LHF cooled the mixed layer by  $5 \text{ W m}^{-2}$  more on average during 2006 compared to 2005, whereas the reduction in surface SWR heating for the same time period is only  $1 \text{ W m}^{-2}$ . The timing of the surface flux and SST differences also suggests a stronger influence from LHF compared to surface SWR. The LHF difference is most pronounced prior to the maximum cold SST difference in June, with LHF cooling the mixed layer by  $11 \text{ W m}^{-2}$  more on average during October 2005–June 2006 compared to October 2004–June 2005. In contrast, surface SWR heated the mixed layer by  $2 \text{ W m}^{-2}$  more on average during October 2005–June

2006 compared to the previous year, opposing the cooling effect of LHF. Finally, the correlation between the 2006 minus 2005 differences in LHF and mixed layer heat storage rate is 0.9 (significant at the 5% level), whereas the correlation between surface SWR and the mixed layer heat storage rate is only 0.1. The high positive correlation between LHF and the heat storage rate suggests that the pronounced cooling leading up to the 2006 hurricane season was driven primarily by LHF.

The SWR measurements at the mooring are affected by the buildup of dust on the radiometer (Medovaya et al. 2002; Foltz and McPhaden 2005). To estimate the magnitude of the effect, we applied a correction to the SWR time series, following Foltz and McPhaden (2005). Application of the correction results in an increase in SWR of  $5\text{--}10\text{ W m}^{-2}$  during July–September 2006, reducing the magnitude of the surface and absorbed SWR difference terms in Fig. 8a. However, this adjustment does not significantly alter our basic conclusions.

The response of SST to changes in surface SWR depends on the depth of the mixed layer as well as the magnitude of the surface SWR,  $Q_{\text{abs}} = Q_{\text{sfc}}(1 - 0.47e^{-h/d_e})$ . During January–August 2006 the mixed layer was generally 10–15 m shallower than during the same period in 2005 (Fig. 8c). As a result, more SWR penetrated through the base of the mixed layer in 2006, tending to decrease the amount of SWR absorbed in the mixed layer. The contrast between surface and absorbed SWR is most pronounced during April–June when the difference in MLD between 2006 and 2005 is greatest. During these months surface SWR was stronger in 2006, coinciding with a reduction in dustiness (Fig. 8a). Indeed, surface SWR tended to heat the mixed layer by  $0\text{--}15\text{ W m}^{-2}$  more during 2006 with respect to 2005. However, because of the increase in SWR penetrating through the base of the mixed layer, absorbed SWR heated the mixed layer by  $10\text{--}20\text{ W m}^{-2}$  less in 2006 relative to 2005. This decrease in absorbed SWR contributed to the weak SST cooling trend during March–June 2006 (Fig. 8).

The amount of SWR penetrating through the base of the mixed layer is also sensitive to the criterion used to define MLD and to the choice of the  $e$ -folding scale for light penetration,  $d_e$ . The choice of MLD criteria has the strongest impact on MLD and absorbed SWR during April–August, when the difference in MLD between 2006 and 2005 is greatest (Figs. 9a,b). The use of a  $0.125\text{ kg m}^{-3}$  criterion instead of  $0.03\text{ kg m}^{-3}$  results in a reversal of the signs of the MLD and absorbed SWR differences during April–June (Figs. 9a,b). These changes have important implications for the heat budget during this period, with differences in absorbed

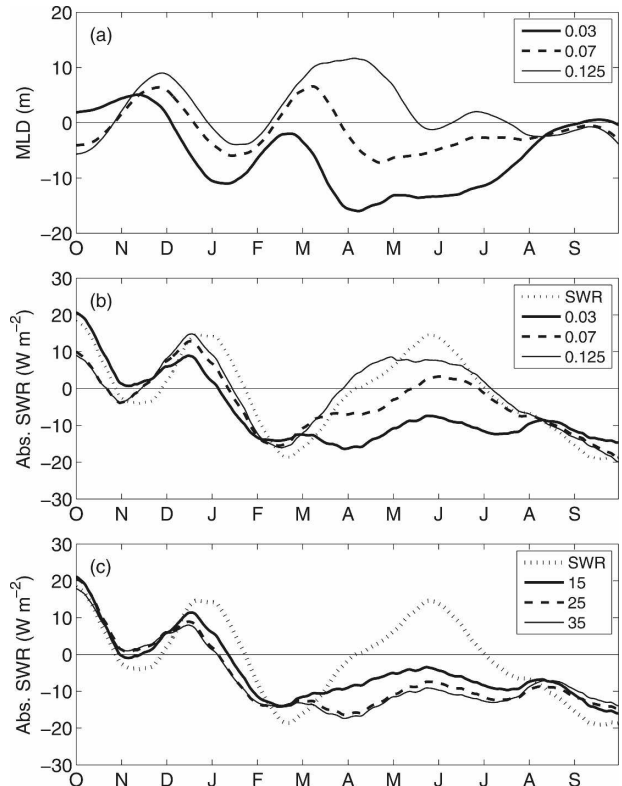


FIG. 9. (a) October 2005–September 2006 minus October 2004–September 2005 differences of MLD at the mooring location using a  $0.03\text{ kg m}^{-3}$  density increase from a depth of 10-m criterion (thick solid), a  $0.07\text{ kg m}^{-3}$  criterion (dashed), and a  $0.125\text{ kg m}^{-3}$  criterion (thin solid). As in (a) but for the amount of SWR absorbed in the mixed layer. Dotted line indicates surface SWR. (c) As in (b) but for a SWR  $e$ -folding depth ( $d_e$ ) of 15 m (thick solid),  $d_e = 25\text{ m}$  (dashed), and  $d_e = 35\text{ m}$  (thin solid), using an MLD criterion of  $0.03\text{ kg m}^{-3}$ .

SWR of up to  $25\text{ W m}^{-2}$ . The use of a deeper MLD criterion also results in a stronger negative correlation between changes in dustiness and absorbed SWR. Changes in  $d_e$  have a relatively minor effect on absorbed SWR in comparison to changes in MLD, with differences of at most  $5\text{ W m}^{-2}$  for  $d_e$  ranging from 15 to 35 m (Fig. 9c). The choices of MLD criteria and  $d_e$  do not alter the basic conclusion from the heat budget analysis, however, which is that changes in SST were driven primarily by LHF.

The sum of LHF, SWR, and horizontal advection explains changes in mixed layer heat storage reasonably well at the mooring location (Fig. 8b). However, there are discrepancies of up to  $15\text{ W m}^{-2}$  that cannot be explained by uncertainties in the terms that we estimated and are likely due partially to our neglect of vertical entrainment/diffusion at the base of the mixed layer, which we cannot estimate directly. There are also uncertainties associated with our horizontal velocity es-

timates, which are averaged in the upper 30 m. These errors are difficult to quantify and are therefore not included in our formal error analysis. They are likely to be most important during January–February when the magnitude of horizontal advection is largest and the MLD is  $>30$  m (Figs. 8a,c).

## 5. Summary and discussion

Our results suggest that Saharan dust exerts a significant influence on surface shortwave radiation (SWR) in the tropical North Atlantic. An increase (decrease) in aerosol optical depth (AOD) is associated with a decrease (increase) in SWR, consistent with previous studies (e.g., Li et al. 2004). The strongest negative AOD–SWR correlations occur in the eastern half of the basin, where interannual variability of atmospheric dust content is high.

Based on statistical analyses we find that AOD-related changes in SWR affect the underlying ocean, with positive (negative) AOD anomalies associated with SST cooling (warming). The relationship is strongest and statistically significant in the central tropical North Atlantic where SWR has the greatest impact on SST. Averaged aerally over the entire tropical North Atlantic ( $10^{\circ}$ – $25^{\circ}$ N,  $20^{\circ}$ – $60^{\circ}$ W), changes in AOD explain  $\sim 35\%$  of the observed SST variability during June–August. A one standard deviation increase (decrease) in AOD during boreal summer is associated with a maximum SST cooling (warming) of  $0.04^{\circ}\text{C month}^{-1}$ .

In the central and western tropical North Atlantic AOD was significantly higher during the early 2006 hurricane season (June–August) in comparison to the early 2005 season, and SST was significantly cooler. Measurements from a long-term moored buoy in the central basin were used to examine the causes of the SST differences. It was found that the cooling was caused primarily by an increase in wind-induced latent heat loss. Variations in surface SWR were negatively correlated with changes in AOD, consistent with the satellite-based results of this study. However, changes in SWR were generally weak in comparison to those of LHF so that dust-induced changes in SWR did not have a strong direct impact on SST.

The results of our historical analysis generally agree with the results of Evan (2007) and Lau and Kim (2007b). Based on the empirical results of Schollaert and Merrill (1998), Evan estimated a AOD-induced reduction in SWR in the western tropical North Atlantic ( $15^{\circ}$ – $30^{\circ}$ N,  $40^{\circ}$ – $70^{\circ}$ W) of  $4\text{ W m}^{-2}$  and an associated SST cooling of  $0.1^{\circ}\text{C}$  in June 2006 with respect to June 2005. Using the same change in AOD (0.05), Lau and Kim estimated a similar reduction in surface SWR and

a resultant SST cooling of  $0.1^{\circ}$ – $0.18^{\circ}\text{C}$ . The difference in cooling rates of Evan and Lau and Kim is due primarily to the use of different mixed layer depths: Evan assumed an average depth of 25 m, whereas Lau and Kim used a range of 15–25 m. Based on the historical analysis in this study, we find that the increase in AOD of 0.05 in June 2006 would have resulted in a reduction in surface SWR of  $3\text{ W m}^{-2}$ , which is similar to the  $4\text{ W m}^{-2}$  estimates of Evan and Lau and Kim. Using an average June mixed layer depth of 27 m for the western tropical North Atlantic (de Boyer Montégut et al. 2007), we estimate SST cooling of  $0.07^{\circ}\text{C}$  in June 2006 compared to June 2005. These results agree with those of Evan and are at the lower end of the estimate given by Lau and Kim.

The analyses of Evan (2007) and Lau and Kim (2007b) are based on the effects of dust on surface SWR and do not take into account the penetration of SWR through the base of the mixed layer. To illustrate how accounting for penetrative radiation would affect their results using the SWR reduction and mixed layer depths that they quote, assume a decrease in surface SWR of  $4\text{ W m}^{-2}$  from a climatological mean value of  $300\text{ W m}^{-2}$  (Zhang et al. 2004) between June 2005 and June 2006. The penetrative component of radiation in this case would be 0.6 and  $1.0\text{ W m}^{-2}$  for mixed layer depths of 25 and 15 m, respectively. These values are 15%–25% of the  $4\text{ W m}^{-2}$  reduction in surface SWR associated with enhanced dustiness and would lead to only a  $0.09^{\circ}$ – $0.13^{\circ}\text{C}$  SST cooling. The results are still consistent with, but lower than, those quoted in Evan (2007) and Lau and Kim (2007b). Evan (2007) and Lau and Kim (2007b) also neglected interannual changes in mixed layer depth, which affect penetrative radiation. We found that the mixed layer was 10 m shallower in the central tropical North Atlantic during June 2006 compared to June 2005, resulting in less SWR available to heat the mixed layer in 2006 despite more surface SWR. These results indicate the importance of considering changes in the penetrative component of radiation when quantitatively estimating the effects of dust on SST.

There are uncertainties associated with our use of satellite-based measurements of SST from infrared sensors, which are affected by the amount of dust in the atmosphere. The aerosol effect would likely lead to an overestimate of the true strength of the dust–SST/SWR relationships. There are also uncertainties associated with the buoy estimates of SWR that are caused by the accumulation of dust on the radiometers. Uncorrected, this effect would likely overestimate the strength of the dust–SWR relationship. The results of this study should therefore be viewed as an upper bound of the effects of

Saharan dust on tropical North Atlantic SWR and SST. Continued satellite measurements of dust, together with satellite-based estimates of SST from microwave sensors and in situ SWR measurements from the PIRATA moorings, will help to better quantify the effects of Saharan dust on the climate of the tropical North Atlantic.

Finally, the results of this study are based on empirical analyses, from which it is difficult to address ultimate causality. For example, it is unclear to what extent changes in dust drive changes in SWR directly (i.e., through the scattering of incoming solar radiation) and to what extent other environmental factors contribute (i.e., humidity and air temperature). It is also unclear how changes in SST feed back to affect atmospheric dust content and whether interannual changes in dust concentration are strong enough to trigger coupled air–sea interactions, as suggested by Lau and Kim (2007a). Examining the results of this study in forced ocean and coupled ocean–atmosphere model simulations would be a valuable next step toward addressing these questions.

*Acknowledgments.* We thank Amato Evan and one anonymous reviewer for their helpful suggestions.

#### REFERENCES

- Bell, G. D., and Coauthors, 2006: The record breaking 2005 Atlantic hurricane season. *Bull. Amer. Meteor. Soc.*, **87**, S44–S45.
- , and Coauthors, 2007: Atlantic basin. *Bull. Amer. Meteor. Soc.*, **88**, S48–S51.
- Bonjean, F., and G. S. E. Lagerloef, 2002: Diagnostic model and analysis of the surface currents in the tropical Pacific Ocean. *J. Phys. Oceanogr.*, **32**, 2938–2954.
- Carton, J. A., X. H. Cao, B. S. Giese, and A. M. daSilva, 1996: Decadal and interannual SST variability in the tropical Atlantic Ocean. *J. Phys. Oceanogr.*, **26**, 1165–1175.
- Chang, P., L. Ji, and H. Li, 1997: A decadal climate variation in the tropical Atlantic Ocean from thermodynamic air–sea interactions. *Nature*, **385**, 516–518.
- Chatfield, R. B., J. A. Vastano, L. Li, G. W. Sachse, and V. S. Connors, 1998: The Great African plume from biomass burning: Generalizations from a three-dimensional study of TRACE A carbon monoxide. *J. Geophys. Res.*, **103**, 28 059–28 077.
- Chiapello, I., J. M. Prospero, J. R. Herman, and N. C. Hsu, 1999: Detection of mineral dust over the North Atlantic Ocean and Africa with the Nimbus 7 TOMS. *J. Geophys. Res.*, **104**, 9277–9291.
- Clark, N. E., L. Eber, R. M. Laurs, J. A. Renner, and J. F. T. Saur, 1974: Heat exchange between ocean and atmosphere in the eastern North Pacific for 1961–71. NOAA Tech. Rep. NMRS SSRF-682, 108 pp.
- Czaja, A., P. Van der Vaart, and J. Marshall, 2002: A diagnostic study of the role of remote forcing in tropical Atlantic variability. *J. Climate*, **15**, 3280–3290.
- de Boyer Montégut, C., G. Madec, A. S. Fischer, A. Lazar, and D. Iudicone, 2004: Mixed layer depth over the global ocean: An examination of profile data and a profile-based climatology. *J. Geophys. Res.*, **109**, C12003, doi:10.1029/2004JC002378.
- , J. Mignot, A. Lazar, and S. Cravatte, 2007: Control of salinity on the mixed layer depth in the world ocean: 1. General description. *J. Geophys. Res.*, **112**, C06011, doi:10.1029/2006JC003953.
- Evan, A. T., 2007: Comment on “How nature foiled the 2006 hurricane forecasts.” *Eos, Trans. Amer. Geophys. Union*, **88**, 271.
- , A. K. Heidinger, and M. J. Pavolonis, 2006: Development of a new over-water advanced very high resolution radiometer dust detection algorithm. *Int. J. Remote Sens.*, **27**, 3903–3924.
- , —, and D. J. Vimont, 2007: Arguments against a physical long-term trend in global ISCCP cloud amounts. *Geophys. Res. Lett.*, **34**, L04701, doi:10.1029/2006GL028083.
- Fairall, C. W., E. F. Bradley, J. E. Hare, A. A. Grachev, and J. B. Edson, 2003: Bulk parameterization of air–sea fluxes: Updates and verification for the COARE algorithm. *J. Climate*, **16**, 571–591.
- Foltz, G. R., and M. J. McPhaden, 2005: Mixed layer heat balance on intraseasonal time scales in the northwestern tropical Atlantic Ocean. *J. Climate*, **18**, 4168–4184.
- , and —, 2006a: Unusually warm sea surface temperatures in the tropical North Atlantic during 2005. *Geophys. Res. Lett.*, **33**, L19703, doi:10.1029/2006GL027394.
- , and —, 2006b: The role of oceanic heat advection in the evolution of tropical North and South Atlantic SST anomalies. *J. Climate*, **19**, 6122–6138.
- , and —, 2008: Seasonal mixed layer salinity balance of the tropical North Atlantic Ocean. *J. Geophys. Res.*, **113**, C02013, doi:10.1029/2007JC004178.
- , S. A. Grodsky, J. A. Carton, and M. J. McPhaden, 2003: Seasonal mixed layer heat budget of the tropical Atlantic Ocean. *J. Geophys. Res.*, **108**, 3146, doi:10.1029/2002JC001584.
- Gentemann, C. L., F. J. Wentz, C. A. Mears, and D. K. Smith, 2004: In situ validation of Tropical Rainfall Measuring Mission microwave sea surface temperatures. *J. Geophys. Res.*, **109**, C04021, doi:10.1029/2003JC002092.
- Giannini, A., R. Saravanan, and P. Chang, 2003: Oceanic forcing of Sahel rainfall on interannual to interdecadal time scales. *Science*, **302**, 1027–1030.
- Goldenberg, S. B., and L. J. Shapiro, 1996: Physical mechanisms for the association of El Niño and West African rainfall with major hurricane activity. *J. Climate*, **9**, 1169–1187.
- , C. W. Landsea, A. M. Mestaz-Nunez, and W. M. Gray, 2001: The recent increase in Atlantic hurricane activity: Causes and implications. *Science*, **293**, 474–479.
- Hastenrath, S., and L. Greischar, 1993: Circulation mechanisms related to Northeast Brazil rainfall anomalies. *J. Geophys. Res.*, **98**, 5093–5102.
- Hsu, N. C., and Coauthors, 1999: Comparisons of the TOMS aerosol index with Sun-photometer aerosol optical thickness: Results and applications. *J. Geophys. Res.*, **104**, 6269–6279.
- Kanamitsu, M., W. Ebisuzaki, J. Woollen, S. K. Yang, J. J. Hnilo, M. Fiorino, and G. L. Potter, 2002: NCEP–DOE AMIP-II reanalysis (R-2). *Bull. Amer. Meteor. Soc.*, **83**, 1631–1643.
- Kaufman, Y. J., and Coauthors, 2005: The effect of smoke, dust, and pollution aerosol on shallow cloud development over the Atlantic Ocean. *Proc. Natl. Acad. Sci. USA*, **102**, 11 207–11 212.
- Kiss, P., I. M. Janosi, and O. Torres, 2007: Early calibration prob-

- lems detected in TOMS Earth-Probe aerosol signal. *Geophys. Res. Lett.*, **34**, L07803, doi:10.1029/2006GL028108.
- Lamb, P. J., 1978: Large-scale tropical Atlantic surface circulation patterns associated with sub-Saharan weather anomalies. *Tellus*, **30**, 240–251.
- Latif, M., N. Keenlyside, and J. Bader, 2007: Tropical sea surface temperature, vertical wind shear, and hurricane development. *Geophys. Res. Lett.*, **34**, L01710, doi:10.1029/2006GL027969.
- Lau, K. M., and J. M. Kim, 2007a: How nature foiled the 2006 hurricane forecasts. *Eos, Trans. Amer. Geophys. Union*, **88**, 105–107.
- , and —, 2007b: Reply to comment on “How nature foiled the 2006 hurricane forecasts.” *Eos, Trans. Amer. Geophys. Union*, **88**, 271.
- Li, F., A. M. Vogelmann, and V. Ramanathan, 2004: Saharan dust aerosol radiative forcing measured from space. *J. Climate*, **17**, 2558–2571.
- Li, X., H. Maring, D. Savoie, K. Voss, and J. M. Prospero, 1996: Dominance of mineral dust in aerosol light-scattering in the North Atlantic trade winds. *Nature*, **380**, 416–419.
- Mahowald, N. M., and L. M. Kiehl, 2003: Mineral aerosol and cloud interactions. *Geophys. Res. Lett.*, **30**, 1475, doi:10.1029/2002GL016762.
- McPhaden, M. J., 2008: Evolution of the 2006–07 El Niño: The role of intraseasonal to interannual time scale dynamics. *Adv. Geosci.*, **14**, 219–230.
- Medovaya, M., D. E. Waliser, R. A. Weller, and M. J. McPhaden, 2002: Assessing ocean buoy shortwave observations using clear-sky model calculations. *J. Geophys. Res.*, **107**, 3014, doi:10.1029/2000JC000558.
- Moisan, J. R., and P. P. Niiler, 1998: The seasonal heat budget of the North Pacific: Net heat flux and heat storage rates (1950–1990). *J. Phys. Oceanogr.*, **28**, 401–421.
- Monterey, G. I., and S. Levitus, 1997: *Seasonal Variability of Mixed Layer Depth for the World Ocean*. NOAA Atlas NESDIS 14, 5 pp.+87 figures.
- Nalli, N. R., and R. W. Reynolds, 2006: Sea surface temperature daytime climate analyses derived from aerosol bias-corrected satellite data. *J. Climate*, **19**, 410–428.
- Prospero, J. M., and T. N. Carlson, 1972: Vertical and areal distribution of Saharan dust over the western equatorial North Atlantic Ocean. *J. Geophys. Res.*, **77**, 5255–5265.
- , and P. J. Lamb, 2003: African droughts and dust transport to the Caribbean: Climate change implications. *Science*, **302**, 1024–1027.
- Remer, L. A., and Coauthors, 2005: The MODIS aerosol algorithm, products, and validation. *J. Atmos. Sci.*, **62**, 947–973.
- Reynolds, R. W., N. A. Rayner, T. M. Smith, D. C. Stokes, and W. Q. Wang, 2002: An improved in situ and satellite SST analysis for climate. *J. Climate*, **15**, 1609–1625.
- Rossow, W. B., and E. N. Dueñas, 2004: The International Satellite Cloud Climatology Project (ISCCP) Web site: An online resource for research. *Bull. Amer. Meteor. Soc.*, **85**, 157–172.
- Saunders, M. A., and A. R. Harris, 1997: Statistical evidence links exceptional 1995 Atlantic hurricane season to record sea warming. *Geophys. Res. Lett.*, **24**, 1255–1258.
- Schollaert, S. E., and J. T. Merrill, 1998: Cooler sea surface west of the Sahara Desert correlated to dust events. *Geophys. Res. Lett.*, **25**, 3529–3532.
- Servain, J., A. J. Busalacchi, M. J. McPhaden, A. D. Moura, G. Reverdin, M. Vianna, and S. E. Zebiak, 1998: A Pilot Research Moored Array in the Tropical Atlantic (PIRATA). *Bull. Amer. Meteor. Soc.*, **79**, 2019–2031.
- Shapiro, L. J., and S. B. Goldenberg, 1998: Atlantic sea surface temperatures and tropical cyclone formation. *J. Climate*, **11**, 578–590.
- Tegen, I., P. Hollrig, M. Chin, I. Fung, D. Jacob, and J. Penner, 1997: Contribution of different aerosol species to the global aerosol extinction optical thickness: Estimates from model results. *J. Geophys. Res.*, **102**, 23 895–23 915.
- Torres, O., P. K. Bhartia, J. R. Herman, Z. Ahmad, and J. Gleason, 1998: Derivation of aerosol properties from satellite measurements of backscattered ultraviolet radiation: Theoretical basis. *J. Geophys. Res.*, **103**, 17 099–17 110.
- , —, —, A. Sinyuk, P. Ginoux, and B. Holben, 2002: A long-term record of aerosol optical depth from TOMS observations and comparison to AERONET measurements. *J. Atmos. Sci.*, **59**, 398–413.
- Wang, W. M., and M. J. McPhaden, 1999: The surface-layer heat balance in the equatorial Pacific Ocean. Part I: Mean seasonal cycle. *J. Phys. Oceanogr.*, **29**, 1812–1831.
- Wentz, F. J., 1997: A well-calibrated ocean algorithm for special sensor microwave/imager. *J. Geophys. Res.*, **102**, 8703–8718.
- Wild, M., and Coauthors, 2005: From dimming to brightening: Decadal changes in solar radiation at Earth’s surface. *Science*, **308**, 847–850.
- Wilks, D. S., 1995: *Statistical Methods in the Atmospheric Sciences*. Academic Press, 467 pp.
- Wong, S., and A. E. Dessler, 2005: Suppression of deep convection over the tropical North Atlantic by the Saharan Air Layer. *Geophys. Res. Lett.*, **32**, L09808, doi:10.1029/2004GL022295.
- Zhang, Y., J. M. Wallace, and D. S. Battisti, 1997: ENSO-like interdecadal variability: 1900–93. *J. Climate*, **10**, 1004–1020.
- , W. B. Rossow, A. A. Lacis, V. Oinas, and M. I. Mishchenko, 2004: Calculation of radiative fluxes from the surface to top of atmosphere based on ISCCP and other global data sets: Refinements of the radiative transfer model and the input data. *J. Geophys. Res.*, **109**, D19105, doi:10.1029/2003JD004457.